Study of eigen frequency $In_{1-x}Gn_xAs_yP_{1-y}$ 1.55 µm VCSEL with SiO_2 /TiO_2 dielectric Bragg reflector

A. Missoum[a,*], N. G. Sabri[b], M. Daoudi[a], H. Guedaouria[a], A. Benamara[c]
[a]*Laboratory of physics and semiconductor devices (LPDS),University of Bechar, P.O.BOX 417, Bechar 08000, Algeria*
[b]*Laboratory of information processing and telecommunication (LTIT), University of Bechar, P.O.BOX 417, Bechar 08000, Algeria*
[c]*Laboratory of Advanced Materials Physical Chemistry (LPCMA), University of Djillali Liabes, BP 89, Sidi-Bel-Abbes 22000, Algeria*

In this work, we focused on investigating the eigen frequency and internal standing wave characteristics of a vertical surface cavity emitting laser operating at a wavelength of 1.55 µm. The design of the cavity involved determining the cavity length, selecting the material for the cavity spacer, and carefully placing the quantum wells within the cavity to achieve maximum overlap with the electric field. In our case, the choice of the dielectric Bragg mirror with SiO_2/TiO_2 layers helps in achieving high reflectivity and low optical losses. The quantum wells are strategically placed within the cavity to ensure maximum overlap with the electric field. This allows for efficient carrier injection and recombination, leading to laser emission. The specific composition of the quantum wells, $In0_{.54}Ga_{0.46}As_{0.99}P_{0.01}$ / $In_{0.75}Ga_{0.25}As_{0.55}P_{0.45}$, indicates the proportions of indium (In), gallium (Ga), arsenic (As), and phosphorus (P) in the material. These compositions are chosen to achieve the desired electronic band structure and emission wavelength. By studying the eigen frequency and internal standing waves in our designed laser cavity, our aim is to understand the resonant modes and behavior of light within the device. This knowledge is crucial for optimizing the laser's performance and improving its efficiency for various applications.

(Received August 15, 2023; Accepted November 1, 2023)

Keywords: VCSEL, dielectric Bragg mirror, Gain, Eigen frequency, 2D axisymmetry

1. Introduction

In the field of telecommunication systems, vertical cavity surface emitting lasers (VCSELs) have gained significant popularity due to their unique properties, including circular beam emission, low threshold current density, and high efficiency in 1.55 µm applications [1]. The use of oxide confined structures in VCSELs has proven to be highly effective in providing both electrical and optical confinement. This enables the demonstration of VCSELs with the highest wall-plug efficiency among VCSELs and the lowest threshold current compared to other semiconductor lasers [2]. In the referenced paper [3], the researchers have demonstrated novel electrically driven vertical cavity surface emitting lasers (VCSELs) operating at 1330 nm and 1550 nm wavelengths. Conventional InGaAsP active regions are used in these VCSELs. The design incorporates two TiO2/SiO2 distributed Bragg reflector (DBR) mirrors and an InAlAs tunnel junction. The VCSEL structure consists of different layers. These layers can have various materials with distinct refractive indices, which are essential for guiding and confining the light within the VCSEL cavity. By considering the refractive index profile of each layer as a function of the radial coordinate r, the Helmholtz equation [4], representing the propagation of light, can be solved in the cylindrical coordinate system [5]. Bienstman and al had done a comparison of optical VCSEL models on the simulation of oxide-confined devices [6]. In our study, $In0_{.54}Ga_{0.46}As_{0.99}P_{0.01}$ / $In_{0.75}Ga_{0.25}As_{0.55}P_{0.45}$ active region is utilized to present electrically driven

* Corresponding author: missoum.asma@gmail.com
https://doi.org/10.15251/JOR.2023.196.607

VCSELs operating at 1550 nm. The VCSELs employ TiO_2/SiO_2 distributed Bragg reflector (DBR) mirrors, 6 pairs on the top and 8 pairs at the bottom. These DBR mirrors are crucial for providing high reflectivity(it can achieve 99.99%) and facilitating optical feedback within the VCSEL cavity. the model used is an eigenfrequency study (VCSEL) that determines the resonant frequency and threshold gain for an oxide-confined. Both electrical and optical confinement are possible with the oxide. As a physical model, we choose a VCSEL setup as described by Bienstman et al. [6].

2. Experimental theory

2.1. VCSEL structure

The VCSEL analysis in cylindrical coordinates (r, ϕ, z). The use of cylindrical coordinates is suitable for modeling the geometry of VCSELs as mentioned in reference [7], which typically have a circular symmetry around the optical axis. In this coordinate system, the variables are defined as follows:

r Radial coordinate, representing the distance from the optical axis., ϕ Azimuthal coordinates, representing the angle of rotation around the optical axis and z Axial coordinate, representing the distance along the optical axis. The model is set up in 2D axisymmetry for the structure in (Figure.1). This means that the structure exhibits symmetry around a central axis, and any properties or fields in the structure do not vary along the axis of symmetry. The modes searched for have an azimuthal dependence of exp(-jϕ), where ϕ is the angle of rotation around the symmetry axis. The description we provided suggests a typical design for an oxide-confined VCSEL, and I'll explain some key components of this structure. The DBR is an essential part of a VCSEL and is responsible for providing optical feedback to create the laser cavity. It consists of alternating layers of materials with high and low refractive indices. These DBR stacks have layers that are each onefourth of a material wavelength thick $d_n=\lambda/4\,n$. The dielectric DBRs must have a very high reflectivity often larger than 99 %. Otherwise, the gain cannot balance the mirror losses.

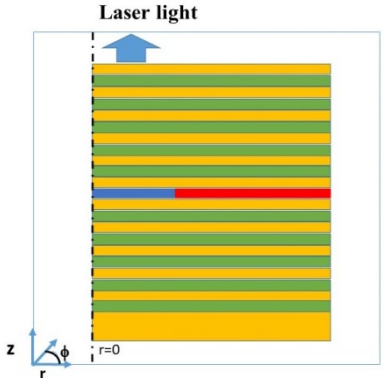

Fig. 1. 2D cross-section of cylindrically symmetric VCSEL (aperture diameter = 6 μm [6]), The top and bottom distributed Bragg reflectors (DBRs) comprise alternating layers of SiO_2 (yellow color) and TiO_2 (green color). The (blue color) central cavity has one quantum well (QW) and, on the top layer an aluminum oxide annular ring(red color).

The structure (see Figure 1) consists of a top and a bottom-distributed Bragg reflector (DBR) structure with alternating high TiO_2 and low refractive index SiO_2 layers. The active material, providing the gain, is located in the cavity between the DBRs. It usually consists of one or more quantum well (QW) layers $In_{0.54}Ga_{0.46}As_{0.99}P_{0.01}$ and the barrier $In_{0.75}Ga_{0.25}As_{0.55}P_{0.45}$. A quantum well layer is a thin layer. the characteristics of each layer are mentioned in (Table 1). VCSEL is designed for operation around 1550 nm. The bottom reflector consists of 8 pairs of SiO2 / TiO_2 , while the top mirror has 6 pairs. In the lower layer of the top mirror, a -thick oxide

aperture is placed. The gain in the 7 nm thick quantum well (QW) is assumed to have a step-index profile with the same dimensions as the oxide aperture. Outside of the aperture, the QW exhibits loss. The structure is grown on a Si substrate.

Table.1. The table resumes the thickness and the refractive index of the used material in the VCSEL.

	thickness	**material**	**Refractive index**
air	/	air	1
6 pair top DBR	269.09nm 158.163 nm	SiO_2 TiO_2	1.44[8] 2.45[8]
Oxide window	15.93 nm	AlOx	1.60 [6]
Cavity	136 nm	SiO_2	1.44
Quantum well	7 nm	$In_{0.54}Ga_{0.46}As_{0.99}P_{0.01}$/ $In_{0.75}Ga_{0.25}As_{0.55}P_{0.45}$	3.5[8]
8 pair bottom DBR	158.163 nm 269.09nm	TiO_2 SiO_2	2.45 1.44

3. Mathematical models

3.1. Threshold gain

The quaternary alloys $In_{0.54}Ga_{0.46}As_{0.99}P_{0.01}$ is used in the quantum well with the gap energy Eg=0.75(eV) and $In_{0.75}Ga_{0.25}As_{0.55}P_{0.45}$ is used in the barrier with Eg=1(eV) to calculate the optical gain . Our study is divided into two models, the first model is the calculation of the optical gain and the second is the calculation of Eigen frequencies. The quantum well of the alloys $In_{1-x}Ga_xAs_yP_{1-y}$ / $In_{1-x}Ga_xAs_yP_{1-y}$. We used the Adachi book and Levenshtein semiconductor handbook [9,10]for the properties of the binary and quaternary alloys injected in our simulation program. Studying the optical gain in a quantum well laser involves a detailed analysis of the laser's characteristics and the interaction between light and matter in the quantum well structure. Here is a general outline of the steps involved: Band structure calculation: Begin by calculating the electronic band structure of the quantum well using appropriate theoretical models, such as the effective mass approximation or the k·p method. This calculation provides information about the energy levels and wave functions of the electrons and holes in the quantum well. The analytical formula for the optical gain in a quantum well laser, as presented by Asada et al. [11]. It provides an approximate expression for the optical gain in a quantum well structure based on several assumptions and simplifications. The formula is given as:

$$g(\omega) = \omega \sqrt{\mu/\varepsilon}\frac{m_{rw}}{\pi}\bar{h}^2 W \sum_{n=0}^{M-1}\int_{E_{cn}+E_{hn}+E_g}^{\infty}\langle R_{ch}^2\rangle \frac{(f_c - f_v)\,\bar{h}/\tau_{in}\, dE_{ch}}{(E_{ch}-\bar{h}\omega)^2 + (\bar{h}/\tau_{in})^2} \qquad (1)$$

Equation (1) is the optical gain analytical formula, which is presented by Asada and al. [11]. Let's break down the components of the formula. $\bar{h}$: Reduced Planck's constant. With ω is the

angular frequency, W is well width, h is plank constant, ε is dielectric constant, μ is vacuum permeability μ=$4\pi \times 10^{-6}$ and m_{rw} is reduit mass in the quantum well. E_{ch} is transition energy, τ_{in} is the inter-band relaxation time and f_c, f_v are fermi functions. M The number of subbands considered in the quantum well. E_{cn}, E_{hn}, E_g: Energy levels of the conduction band, valence band, and bandgap, respectively, in the quantum well. ⟨Rch⟩ the dipole moment. The formula involves integration over energy (E_{ch}) in the conduction band, starting from the dipole moment, sum of energy levels E_{cn}, E_{hn}, and E_g up to infinity. The integrand consists of terms related to the carrier distribution functions, and the energy dependent term in the denominator.

$$E_{in} = \frac{\left[\frac{(n+1)\pi}{2}\frac{a_i}{(W+\Delta W_i)}\right]^2}{\left[1+\left\{\frac{(n+1)\pi}{2}\right\}^2 b_i\left(\frac{\Delta W_i}{W+\Delta W_i}\right)^3\right]} \tag{2a}$$

$$\Delta W_i = \frac{a_i}{\sqrt{b_i \Delta E_i}}, \quad a_i = \frac{2\bar{h}}{\sqrt{2m_{iw}}} \; and \; b_i = \frac{m_{iw}}{m_{ib}} \tag{2b}$$

The quantized energy Equation (2a) is based on a simple parabolic band by introducing theoretical expressions introduced by Makino [12]. Where in Equation (2b) the subscripts i is (c or h) conduction band or heavy hole valence band respectively and n = 1, 2, 3… Denote the number of the quantized level (or the subband, in other words) in the well, respectively. m_{iw} is the mass of the electron or hole in the well and m_{ib} in the barrier.

3.2. The electric wave equations

The wave equation electric is related to the quantity's second derivative in time to its second derivative in space (Equation.3). In the context of electromagnetic waves in a source-free region (ρv=0 and $\bar{J}$=0), the electric wave equation can be derived from the combination of Ampere's Law and Faraday's Law, Therefore the electric wave equation

$$\nabla \times \left(\frac{1}{\mu_r}\nabla \times \vec{E}\right) - k_0^2 \varepsilon_{rc} \vec{E} = 0 \tag{3}$$

In a 2D axisymmetric scenario, (Equation.4) where the electric field varies with the azimuthal mode number m, the correct expression for the electric field can be written as:

$$\vec{E}(r, \varphi, z) = \vec{E}(r, z) e^{-im\varphi} \tag{4}$$

Here(Equation.4), E(r, φ, z) represents the electric field vector in cylindrical coordinates [13], which depends on the radial coordinate r, the azimuthal angle φ, and the spatial coordinate along the propagation direction z. E (r, z) represents the magnitude and direction of the electric field vector at each point in the r-z plane, and exp(-imφ) represents the azimuthal dependence of the field. The term exp(-imφ) represents a complex exponential function that describes the phase and amplitude variation of the electric field in the azimuthal direction. The factor m determines the mode number and influences the spatial distribution of the field. The azimuthal dependence is periodic with a period of 2π/m, meaning that the field repeats itself after a full revolution of 2π/m radians. By incorporating this azimuthal dependence, the expression captures the behavior of the electric field in a system with rotational symmetry around the z-axis. For the 2D axisymmetric

case where the electric field (Equation.5) varies with the azimuthal mode number m, the wave equation can be written as:

$$\left(\nabla - i\frac{m}{r}\varphi\right) \times \left[\frac{\left(\nabla - i\frac{m}{r}\varphi\right)}{\mu_r} \times \vec{E}\right] - k_0^2 \varepsilon_{rc} \vec{E} = 0 \quad (5)$$

Here, ∇ represents the gradient operator, $(\nabla - i\frac{m}{r}\varphi)$ represents the derivative operator in the azimuthal direction, φ represents the unit vector in the out of plane direction. μ_r represents the relative permeability, ε_{rc} represents the relative permittivity, k_0 represents the wave number $k_0=\omega\sqrt{\varepsilon_0\mu_0}=\frac{\omega}{c_0}$ And $\vec{E}$ represents the electric field vector.

The term $\left(\nabla - i\frac{m}{r}\varphi\right) \times \left[\frac{\left(\nabla - i\frac{m}{r}\varphi\right)}{\mu_r} \times \vec{E}\right]$ represents the curl of the curl of the electric field, taking into account the azimuthal derivative $\left(\nabla - i\frac{m}{r}\varphi\right)$and the vector cross product $\left[\frac{\left(\nabla - i\frac{m}{r}\varphi\right)}{\mu_r} \times \vec{E}\right]$.

The wave equation states that this expression should be equal to the product of $k_0^2\varepsilon_{rc}$ and the electric field vector $\vec{E}$, ensuring that the electric field satisfies the wave equation. This equation describes the behavior of the electric field in a 2D axisymmetric system, considering both the spatial variation and the azimuthal mode number m. Solving this wave equation allows for the determination of the electric field distribution and its dependence on the radial coordinate r, the azimuthal angle φ, and the spatial coordinate z.

4. Results and discussion

4.1. The calculation of the optical gain

In quantum wells, the optical gain is computed with the previous equations (1 and 2). We can notice that our results agree well with Makino's results (Figure 2. a) and almost all the picks are a round of 1.55µm. We choose the addition of y=0.01% of phosphor in the quaternary alloy InGaAsP lattice-matched with the barrier. So, according to these results, we have extracted the characteristic of the quantum of such as the optical threshold gain g=2100cm^{-1} at the pick of 1.55µm and the width of Quantum Well d= 7nm.

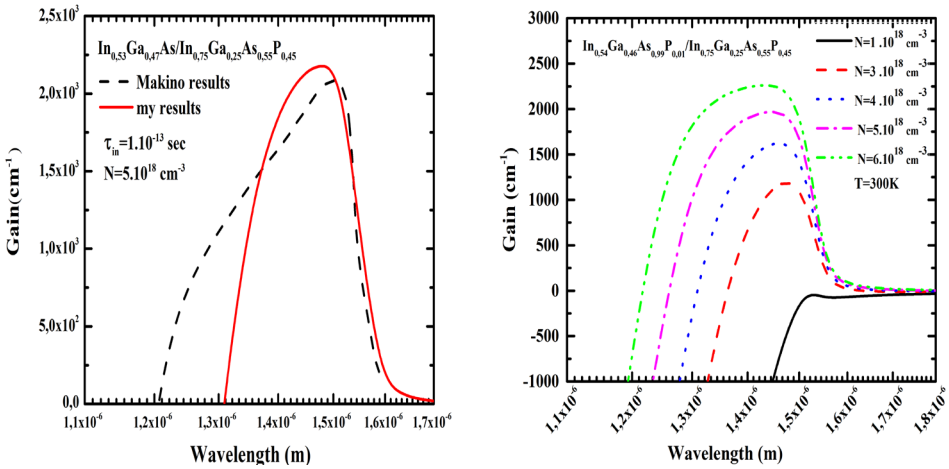

Fig. 2. the optical gain (a) the validation of the work with Makino results [12], (b) Optical gain of the strained MQW active region as a function of the wavelength with various carrier densities as parameters (T=300 K).

4.2. VCSEL simuation (Eigen frequency calculation)

The extracted characteristics from the previous results the pick of threshold gain at 1.55µm and the parameters in (Table 1) are injected into the Eigen frequency study using the equations 4 and 5 to get the results in Figure 3. The mode is confined essentially between the top and the bottom DBRs. To calculate frequency simply, we use the following formula: f= $^{c}/_{\lambda}$. With c is the Light speed and λ is the wavelength. Therefore, 193.54 Thz is the frequency that corresponds to wavelength 1.55 µm. Just in case, the value is fixed. The outcomes are in line with The result after the second (nonlinear) Eigen frequency study shown in (Figure 3)which provides a summary of the resonance wavelength λ≈ 1.554µm and the Eigenfrequency f≈193+0.77103i Thz. The surface electric field intensity is maximum it achieved 12.3 V/m in the middle of the cavity . This results from the fact that the wavelength of this mode most closely matches the peak of the gain spectrum.

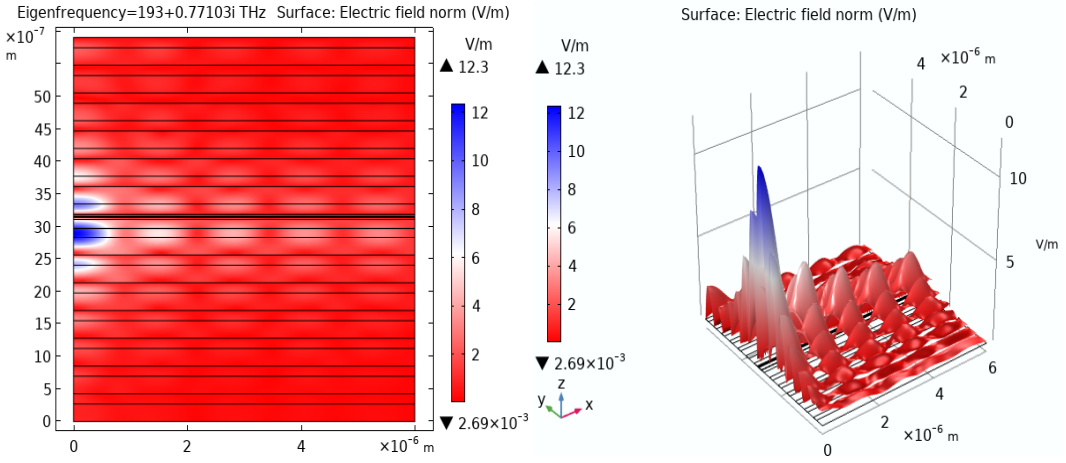

Fig. 3. (a) Surface plot of the mode field after the initial Eigen frequency study. The plot shows the norm of the electric field, with the symmetry axis at r = 0.; (b) shows the mode field after the initial Eigenfrequency study.

5. Conclusions

The longitudinal resonator modes, or electric field distributions, resulting in a standing wave in the cavity, depending on the length of the resonator cavity. A beam's form is determined by its modes. After completing one closed loop path inside the resonator, these modes continue to exist and repeat themselves (aside from potentially losing some power due to loss in the cavity). The resonator cavity, a laser optical mirror, in which the laser light is amplified in a gain medium, controls the form of a laser beam. In order to avoid light from escaping, laser resonators are often built using monolithic crystals or highly reflecting dielectric mirrors in this case (TiO_2/SiO_2). The highest electric field intensity (E=12.3V/m) is maximum in the middle of the resonator cavity. This results from the fact that the wavelength of this mode most closely matches the peak of the gain spectrum at $g=2100cm^{-1}$.

Acknowledgments

This work is supported by the algerian ministry of higher education and scientific research under the PRFU programm, project A25N01UN080120200002.

References

[1] O.Conradi, P.Reinhold, Optical and Quantum Electronics 32(6), 767(2000); https://doi.org/10.1023/A:1007058210442

[2] I.Kenichi, IEEE Journal of Selected Topics in Quantum Electronics 6(6),1201 (2000); https://doi.org/10.1109/2944.902168

[3] W.C.Weng, D.C.Kent, H.C.Mary, L.L.Kevin, G.H.Ronald, IEEE Journal of Quantum Electronics 33(10), 1810(1997); https://doi.org/10.1109/3.631287

[4] M.R.Virginia, D.L.Steven, P.B.David, N.M.Jeffrey, M.Francoise, Physics and Simulation of Optoelectronic Devices XII 5349, 366(2004); https://doi.org/10.1117/12.540323

[5] S.Foad, Conference: 3rd.International Conference on Researches in Science & Engineering, 2017.

[6] C.Olaf, P.Reinhold, Optical and Quantum Electronics 32(6), 759(2000); https://doi.org/10.1023/A:1007058210442

[7] B.Peter, B.Roel, V.Josip, L.Anders, N.Michael J, B. Marcel, G.Karlheinz, D.Pierluigi, F.Laura, P.B.Gian, W.Hans, K.Benjamin, C.Olaf, P.Reinhold, A.R.Spilios, P.S.Jean-François, L.C. Shun IEEE Journal of Quantum Electronics 37 (12), 1618(2001); https://doi.org/10.1109/3.970909

[8] G.H.Ronald, L.L.Kevin, M.E.Warren, D. C.Kent, J.W.Scott, C.Scott, IEEE Journal of Quantum Electronics 32(4), 607(1996); https://doi.org/10.1109/3.488833

[9] P.Joachim , W.Hans, W.Hans-Juergen, D. Braun, H.Fritz, Physics and Simulation of Optoelectronic Devices III 2399, 605(1995); https://doi.org/10.1117/12.212533

[10] A.Sadao, "Properties of Semiconductor Alloys: Group-IV, III-V and II-VI Semiconductors",

John Wiley and Sons Ltd, 400, 2009; https://doi.org/10.1002/9780470744383

[11] L.E.Mikhail, L.R.Sergey, and S.Michael, Handbook Series on Semiconductor Parameters Volume 2, Singapore: World Scientific, 220, 1996.

[12] A.Masahiro, A.Kameyama, S.Yasuharu, IEEE Journal of Quantum Electronics 20(7), 753(1984); https://doi.org/10.1109/JQE.1984.1072464

[13] M.Toshihiko, IEEE Journal of Quantum Electronics 32(3), 501(1996); https://doi.org/10.1109/3.485401